Compatibility of materials for macroencapsulation of inorganic phase change materials: experimental corrosion study

Svetlana Ushak[1,2,*], Paula Marín[1], Yana Galazutdinova[1], Luisa F. Cabeza[3], Mohammed M. Farid[4], Mario Grágeda[1,2]

[1]*Department of Chemical Engineering and Mineral Processing, and Center for Advanced Study of Lithium and Industrial Minerals (CELiMIN), Universidad de Antofagasta, Campus Coloso, Av.Universidad de Antofagasta, 02800 Antofagasta, Chile*

[2] *Solar Energy Research Center(SERC-Chile), Av Tupper 2007, Piso 4, Santiago, Chile*

[3] *GREA Innovació Concurrent, Universitat de Lleida, Edifici CREA, Pere de Cabrera s/n, 25001, Lleida, Spain*

[4] *Department of Chemical and Materials Engineering, The University of Auckland, Private Bag 92019, Auckland 1142, New Zealand*

Corresponding author: Svetlana Ushak, e-mail: svetlana.ushak@uantof.cl, tel. 56-552637313, fax 56-552637801

Abstract

The potential of the use of salt hydrates $MgCl_2 \cdot 6H_2O$ (bischofite) with typical impurities of the Salar de Atacama as a thermal energy storage material was evaluated with special attention to its corrosion behavior. Bischofite behavior is compared with that of commercial salt $MgCl_2 \cdot 6H_2O$. The corrosion tests were conducted with metal sheets (copper, aluminum and stainless steel) partially immersed in molten salt hydrates at a temperature of 120°C during 1500 hrs. The results showed minimum corrosion on all the immersed surfaces of all the metals. However, very sever corrosion was observed at the salt/air interface due to a known phenomenon of oxygen enhanced corrosion usually found even with water at ambient temperature. The corrosion products were determined with scanning electron microscopy (SEM) and X-ray diffraction (XRD) technique. For salts hydrates bischofite and $MgCl_2 \cdot 6H_2O$, the results show the formation of cuprite (Cu_2O) and hematite (Fe_2O_3) on copper and stainless steel samples, respectively. For all cases studied in the present work, several chloride compounds were identified as corrosion products.

Keywords: *phase change materials; salt hydrates; interface corrosion; bischofite*; $MgCl_2 \cdot 6H_2O$

1. Introduction

One of the most promising technologies of thermal energy storage is using of latent heat, which employs a phase change material (PCM) as the energy storage medium [1,2]. The principle of a PCM is as follows: as the temperature of the medium increases, the material absorbs heat through melting, minimizing changes in the surrounding temperature. Similarly, when the temperature of the medium decreases, the PCM changes from liquid phase to solid, releasing heat and thereby minimizing the decrease in surrounding temperature [3,4]. Due to the fact that absorption and release of heat of fusion is associated with the formation of a liquid phase, it is necessary to encapsulate the PCM to prevent its leakage [5]. Since these salts in their liquid state are able to cause corrosion, it is necessary to evaluate the impact of these PCMs and their impurities on the compatibility with the materials of the containment capsules [6-13]. PCMs can be used in different applications, being solar energy one of the most promising ones, as published by Esen and Ayhan [14], Esen et al. [15], Esen [16], Cabeza et al. [17], Mazman et al. [18], and Gil et al. [19].

PCMs are categorized as eutectic, organic and inorganic materials. A eutectic material is a composition of two or more components forming a mixture having congruent melting and solidification. Organic PCM materials, classified into paraffins and non-paraffins are considered to be non-corrosive and highly stable. Meanwhile, the inorganic PCM are classified as salt hydrates and salts. These inorganic compounds have a high latent heat per unit weight, being inexpensive compared to organic compounds, non-flammable and readily available [20-24]. It is for this reason that this study focuses on the use of inorganic materials as a thermal storage medium. Salt hydrates, in particular, have demonstrated appropriate chemical storage stability [7], and positioned themselves as a perspective PCM. They are also an abundant resource in many areas worldwide, but especially in northern Chile.

Northern Chile has a unique potential for the development and implementation of clean energy technologies. The climatic conditions of this region represent an opportunity for the development of clean technologies based on the use of solar energy. Moreover the large reserves of salts found in the Salar de Atacama and other salt lakes, provide the materials needed to store the captured solar energy [25]. The Salar de Atacama, located

in Region II of Chile, is the main reservoir, at the continental level, for natural magnesium chloride hexahydrate ($MgCl_2 \cdot 6H_2O$), also known as bischofite.

Bischofite ($MgCl_2 \cdot 6H_2O$) is an attractive material to be used as storage material for thermal energy because it has moderate heat of fusion (168 kJ/kg) and reasonable thermal conductivity (about 0.570 W/(m·K)) as well as having low cost compared with most organic PCMs [26].

Previously, Ushak et al. [26] performed physical characterization of the thermal properties of natural bischofite, focusing on their suitability as a phase change material. The properties exhibited by natural bischofite showed its suitability for use as a PCM, therefore, the next step would be to generate a methodology for its encapsulation for use in a number of applications.

The objective of the work presented is to assess the potential of salts hydrates bischofite (based on $MgCl_2 \cdot 6H_2O$ with typical impurities; hereinafter bischofite will refer to the salt and impurities) of the Salar de Atacama, for use as a thermal energy storage material by testing its corrosion behavior. Bischofite corrosion behavior will be compared with that of commercial $MgCl_2 \cdot 6H_2O$, a well-known PCM [26]. The compatibility and corrosion resistance of encapsulating materials such as copper, aluminum and stainless steel, at a temperature of 120°C for extended periods is studied and analyzed.

Corrosion of $MgCl_2 \cdot 6H_2O$ as used in TES has not been previously evaluated in details. Nagano et al. [9] studied the corrosion of $Mg(NO_3)_2 \cdot 6H_2O$ against six metals and its mixture with $MgCl_2 \cdot 6H_2O$ against aluminum. Their results showed that aluminum can be used to encapsulate the mixture of $Mg(NO_3)_2 \cdot 6H_2O$ + 10% $MgCl_2 \cdot 6H_2O$. While El-Sebaii et al. [27] carried out compatibility tests of aluminum and stainless steel embedded in $MgCl_2 \cdot 6H_2O$ and found strong corrosion in both cases. Therefore, since no detailed study of the corrosion of $MgCl_2 \cdot 6H_2O$ has been carried out previously in the literature, it will be included in this paper for comparison purposes.

2. Materials and methods

2.1 Materials

As in previous investigations [7,8], three different base metals with an extensive use in the Chilean industry were used in this research. These metals were copper, aluminum and stainless steel. Their characteristics are given in the Table 1.

Table 1.

Bischofite (composed primarily of $MgCl_2 \cdot 6H_2O$) was obtained from brine evaporation ponds located in the salt mines at different times of the year and according to chemical analysis, has a purity of 94.80% (Table 2) [26]. Commercial $MgCl_2 \cdot 6H_2O$ was purchased from Merck (> 99% purity). Their properties are shown in the Table 3.

Table 2.

Table 3.

2.2 Methods

2.2.1 Corrosion measurements

Although corrosion data of salts solutions in water is available from the chemical industry and literature, they are not available for these salts to be used as PCMs (i.e. in solid state) and especially at the required high temperatures. Producing new corrosion data is essential for PCM utilization in new applications. Following this idea, Cabeza et al. [7,8], Moreno et al. [10] and Oró et al. [21] studied the corrosion resistance of metals and metal alloys in contact with different salt hydrates. In these studies, corrosion tests were carried out with the metal sample fully immersed in the melted PCM, similarly to those of Nagano et al. [9] and El-Sebaii et al. [27]. However, TES tanks usually are never filled to their maximum capacity due to the known volume change of the PCM when undergoing heating and cooling cycles; therefore an air-liquid-interface (ALI) is usually expected in most storage systems. ALI corrosion is a well-known phenomenon at the air-liquid-interface region on a partially-immersed metal surface [28]. Literature

reports that ALI corrosion can appear in pairs that do not show corrosion in fully-submerged metal surfaces [28,29]. Although the mechanism of ALI corrosion is still not well understood [28,30,31], some authors relate it to the dissolved oxygen at the air-liquid interface [32,33].

In this study, five samples of each metal were used with bischofite and another five samples with the pure salt $MgCl_2 \cdot 6H_2O$ (see Figure 1). The size of the samples was 50×30×0.1 mm for copper and aluminum as shown in Figure 2. Samples of 316L stainless steel were of 50×30×3 mm in size. The initial mass of each sample was recorded to observe the behavior of mass loss through time.

Figure 1.

Figure 2.

Salts of a certain mass (bischofite and pure $MgCl_2 \cdot 6H_2O$) were placed in separate borosilicate glasses and were molten at 120°C in a muffle furnace, the height of the molten salt in the glass containers was 2 cm. The metal samples were placed in the borosilicate glass container in such a way that 50% of its surface was immersed in the salt solution (see Figure 1).

Figure 3 shows a schematic representation of the oven cavity to which the glass container containing molten salts with metal samples was introduced.

Figure 3.

Corrosion tests were performed as follows: samples were removed from the oven at different times, sample Nº1 (250 hrs), sample N°2 (500 hrs), sample Nº3 (750 hrs), sample Nº4 (1000 hrs), and finally sample Nº5 (1500 hrs). Once removed, the samples were washed with distilled water to remove residual soluble compounds and then were placed in an oven at 55°C for two hours to remove residual moisture. Based on the previous methodology used [10], data obtained from the experimentation were further evaluated. Mass loss (g) was calculated with Eq. (1), considering the initial mass, $m(t_0)$, and the mass measured after 250, 500, 750, 1000 and 1500 hrs, m(t), respectively:

$$\Delta m = m(t_0) - m(t) \qquad \text{Eq.(1)}$$

2.2.2 XRD and SEM-EDX analyzes of samples with corrosion products

Once the exposure of the metal samples in salts was concluded, the corrosion products were subjected to XRD and SEM-EDX analyzes to evaluate the chemical composition and differential patterns of corrosion.

A scanning electron microscope (SEM) Jeol, Model JSM6360 LV coupled to an energy dispersive X-ray spectrometer (EDX) Inca Oxford was used to analyze the morphology and composition of metal samples with corrosion products.

The mineral composition of products, formed as result of the corrosion, was analyzed through X-Ray Powder Diffractometer. The powdered samples were positioned on a flat plate sample holder and the analysis was performed on a X-Ray diffractometer SIEMENS model D5000 (40 kV, 30 mA); radiation of Cu Kα1 (λ = 1.5406 Å); vertical Bragg-Brentano; scan range: 3 - 70° 2θ; step size: 0.020° 2θ; step time: 1.0 s.

3. Results

3.1 Corrosive effect of salts hydrates on metals, in relation to mass loss

Mass loss was considered as a variable to evaluate the corrosive effect of two salt hydrates (bischofite and $MgCl_2 \cdot 6H_2O$) on three types of metals (copper, aluminum and stainless steel).

Mass loss of copper samples against salts

Copper was the metal that was most affected by the corrosive effect of salts (see Section 3.2). This is why it was not possible to determine the final mass loss due to the complete fragmentation of both samples (of commercial salt and bischofite) (Figure. 4).

Mass loss of aluminum samples against salts

Aluminum and stainless steel samples were able to complete the exposure period. In this case, aluminum is the metal which shows the greatest mass loss in both treatments with a total mass loss of 8.34% in the treatment with $MgCl_2 \cdot 6H_2O$ (Merck) and 10.70-12.21 % in the treatment with bischofite (Table 4). It is important to note that aluminum has a greater mass loss under the treatment with commercial salt (Figure 5, Table 4).
Figure 5 also shows the aluminum from the period of 500 hours of treatment shows a mass gain, which is probably due to the formation of a stable layer of aluminum oxide which could not be removed in the evaluation period of the experimetation. However, the behavior is different from aluminum in contact with the molten salt bischofite: there is a stable mass loss until 500 hours of treatment. After this time, the aluminum foil is broken by corrosion right at the interface air-molten salt.

Mass loss of stainless steel samples against salts

Stainless steel is the metal showing the least mass loss in all cases tested, with a total mass loss of 0.32% for treatment with $MgCl_2 \cdot 6H_2O$ and 0.44% for treatment with bischofite (Figure 6, Table 4).

Figure 4.

Figure 5.

Figure 6.

Table 4.

The determination of mass loss used as an indicator of the corrosive effect indicates that stainless steel was the most resistant to bischofite and commercial $MgCl_2 \cdot 6H_2O$. In the case of aluminum, although it shows less degradation, increased mass loss is revealed when compared with stainless steel samples.

In previous studies the effectiveness of the application of both steel and aluminum due to their resistance to corrosion has been highlighted [7,8]. In the first of these studies, it

is concluded that both stainless steel and aluminum are recommended for their use in encapsulation, having a lesser degree of corrosion of <0.2 mg/cm^2·yr in both cases [7]. However, the later work [8] concludes that aluminum is the metal which has the highest degree of corrosion, taking into account not only the corrosion rate but also visual changes in the solution and the metal, in addition to changes of pH. In both studies metals are tested under different conditions, so in these cases it is important to consider the test medium in which it is desired to determine the degree of corrosion of each metal.

A similar study was performed by Nagano et al. [9], who carried out a number of corrosion tests in a particular environment and determined that the metals recommended to be used in storage tanks were SUS316 stainless steel and aluminum.

As described in previous works, aluminum and stainless steel are materials that exhibit corrosion resistance and have been nominated as materials for PCM encapsulating. However, mass loss is not a conclusive parameter of corrosive effect due to the formation of various impurities and protective oxide layers that cannot be easily removed during the evaluation period. The phenomenon is evident in the case of stainless steel.

The presence of impurities in salts has been previously described as the factor that could positively or negatively influence the corrosion of metals. In the case of having a negative effect on the corrosion, in other words, retarding the corrosion process, this phenomenon is denoted as metal passivation [35]. In the case of stainless steel, it is likely that the phenomenon occurring is passivation, because the results of fitness (qualitative observation) show a typical oxide layer, however, measurements of mass loss indicate no destructive effect corrosive on the metal sample, a process which was not observed in the case of aluminum.

3.2 Corrosion of metals by salt hydrates

Tables 5 and 6 present a summary of physical conditions of three studied metals, treated with molten salts during different periods of time.

Table 5.

Table 6.

Tables 5 and 6 show that copper is poorly represented, with aluminum and stainless steel following. The copper sample has broken at the interface before the final point of the experiment. The formation of blue and green compounds on the sample corresponds to chlorinated compounds and oxidized copper, during the treatment with both bischofite and the commercial salt.

Something similar occurred with stainless steel where the metal suffers from the degradation related to the oxidation process typical for this metal. In the case of aluminum, the effect of physical degradation with clear signs of detachment was more apparent in the case of treatment with bischofite, which was not observed in the case with commercial salt.

As it can be seen in Figure 7, in the case of stainless steel and copper, there is a highlighted oxidative effect in the interface area (i) molten salt-air, where a physical deterioration of the material is initially perceived followed by an accumulation of residues from the oxidative process.

Figure 7.

3.3 XRD analysis of the corrosion products

In Figures 8 and 9, the diffractograms of XRD analysis for the metal sheets exposed to salts bischofite and $MgCl_2 \cdot 6H_2O$, respectively, are presented. Based on Figure 8, there is no common pattern of compounds forming the corrosion product. Figure 9 also shows no common pattern between the metal sheets treated with bischofite.

Figure 8.

Figure 9.

Results show that between samples of the same type (i.e. copper sheet treated with $MgCl_2 \cdot 6H_2O$ and bischofite) there is a correlation between some of the compounds constituting the corrosion product. In this case, cuprite is the common compound between the copper sheets treated (Cu_2O). The same applies to the case of stainless steel where the common product of corrosion is hematite (Fe_2O_3). While the product for the case of aluminum immersed in bischofite was not identified since it was an amorphous compound. The summary of phase identified by XRD is presented in Table 7.

Table 7.

For aluminum in contact with $MgCl_2 \cdot 6H_2O$, the corrosion products show that both the cation (Mg^{2+}) and the anion (Cl^-) react with the metal (Al) forming new compounds (Table 5). When copper and stainless steel are immersed in $MgCl_2 \cdot 6H_2O$, reaction between the anion (Cl^-) and the metal (Cu or Fe) was observed, indicating different corrosion mechanisms.

For all cases studied in the present work (three metal samples and two hydrate inorganic compounds) chloride compounds were formed (see the Table 5). Also, for copper and iron metal sheet, Cu_2O and F_2O_3 oxides were observed.

3.4 SEM-EDX analysis of the corrosion products

Figure 10 shows SEM images for three metals in contact with bischofite for 250 hrs.

Figure 10.

The part of stainless steel and aluminum sheets immersed in the salts did not show any corrosion after 250 h of treatment. But the areas near the interface show severe corrosion (darker colors). The copper sample shows partial breaking at the interface. In this case, the immersed area shows isolated products of corrosion. EDX analysis results for the metals in contact with bischofite are shown in Table 8. Here, no important differences are seen between interface or immersed area for the same metal.

Table 8.

To analyze the progress of corrosion with time, the results for aluminum sheets after 250 h and 1500 h of treatment are shown in Figure 11.

Figure 11.

After 250 h, a partial breakage of the metal in the interface can be seen. Moreover, corrosion products (dark color) appear on the surface of the cleaned sheets both at 250 and 1500 h. On the other hand, the immersed part shows no differences in the exposed samples during the different time periods, with relatively low corrosion in the form of pitting pattern.

4. Comparison with previous published research

The published data indicate that there is a lack of corrosion studies of effects of magnesium chloride hydrate alone on metals [7-10,27]. Moreover, no work has been published about corrosion behavior of molten bischofite. Some researchers used mass loss to determine corrosion rate. Table 9 summarizes the published results from those studies and the results presented in this work.

Table 9.

The work presented in this paper shows that the corrosion behavior of bischofite follows the same pattern of that of magnesium chloride hexahydrate, but in the case of bischofite the corrosion is higher, probably due to the presence of various impurities in this salt. Similar conclusion can be drawn by comparing the results presented here with those of magnesium chloride hexahydrate published earlier [27]. On the other hand, previous published results of mixtures of magnesium chloride hexahydrate show better corrosion performance than those presented here. Finally, the impurities found in bischofite (Table 2) have not been considered in any of the previously studied mixtures, so no comparison can be made.

5. Conclusions

Compatibility of bischofite as PCM needed to be encapsulated was studied with three different metal samples: copper, aluminum and stainless steel. The results were compared with those obtained when commercial magnesium chloride hexahydrate was used.

The corrosion products were determined by XRD technique. For hydrate salts bischofite and $MgCl_2 \cdot 6H_2O$, the results show that cuprite (Cu_2O) and hematite (Fe_2O_3) are compounds formed on copper and stainless steel samples, respectively. Also, for all cases studied, several chloride compounds were identified as corrosion product.

This study showed minimum corrosion occurred on all the immersed surface of all the metals. However, very sever corrosion occurred at the salt-air interface due to a well-known phenomena of oxygen enhanced corrosion usually found even in water tanks at ambient temperature. This suggests that care should be taken in the design of these heat storage systems to avoid completely the presence of air, otherwise the storage unit could fail in a very short period. Further studies of the corrosion process in inert atmosphere and under different conditions are suggested to identify the trigger of corrosion in the interface.

Acknowledgements

The authors would like to acknowledge the collaboration of the company SALMAG. The authors acknowledge to CONICYT/FONDAP Nº 15110019, and the Education Ministry of Chile Grant PMI ANT 1201 for the financial support. P. Marin thanks fellowship CONICYT-PCHA/doctorado nacional/2015-21151359. Y.Galazutdinova thanks fellowship CONICYT-PCHA Nº 63140052. This work was partially funded by the Spanish project ENE2011-22722. Dr. Luisa F. Cabeza would like to acknowledge the Generalitat de Catalunya for the quality recognition 2014-SGR-123. The research leading to these results has received funding from the European Commission Seventh Framework Programme (FP/2007-2013) under grant agreement N° PIRSES-GA-2013-610692 (INNOSTORAGE).

References

[1] Kousksou T, Bruel P, Jamil A, El Rhafiki T, Zeraouli Y. Energy storage: Applications and challenges. Solar Energy Materials & Solar Cells 2014;120:59-80.

[2] Tatsidjodoung P, Le Pierrès N, Luo L. A review of potential materials for thermal energy storage in building applications. Renewable and Sustainable Energy Reviews 2013;18:327-349.

[3] Feldman D, Shapiro M.M, Banu D, Fuks C.J. Fatty acids and their mixtures as phase-change materials for thermal energy storage. Solar Energy Materials 1989;18 (3-4):201-216.

[4] Felix Regin A, Solanki S.C, Saini J.S. Heat transfer characteristics of thermal energy storage system using PCM capsule: A review. Renewable & Sustainable Energy Reviews 2008;12(9):2438-2458.

[5] Schossing P, Henning H-M, Gschwander S, Haussmann T. Micro-encapsulated phase-change materials integrated into construction materials. Solar Energy Materials & Solar Cells 2005;89(2-3):297-306.

[6] Salunkhe Pramod B, Shembekar Prashant S. A review on effect of phase change material encapsulation on the thermal performance of a system. Renewable and Sustainable Energy Reviews 2012;16(8):5603-5616.

[7] Cabeza L.F, Roca J, Nogués M, Mehling H, Hiebler S. Immersion corrosion test on metal-salt hydrate pairs used for latent heat storage in the 48 to 58°C temperature range. Materials and Corrosion 2002;53(12):902-907.

[8] Cabeza L.F, Roca J, Nogués M, Mehling H, Hiebler S. Long term immersion corrosion test on metal-PCM pairs used for latent heat storage in the 24 to 29°C temperature range. Materials and Corrosion 2005;56(1):33-39.

[9] Nagano K, Ogawa K, Mochida T, Hayashi K, Ogoshi H. Performance of heat charge/discharge of magnesium nitrate hexahydrate and magnesium chloride hexahydrate mixture to a single vertical tube for latent heat storage system. Applied Thermal Engineering 2004;24 (2-3):209-220.

[10] Moreno P, Miró L, Solé A, Barreneche C, Solé C, Martorell I, Cabeza L.F. Corrosion of metal and metal alloy containers in contact with phase change materials (PCM) for potential heating and cooling applications. Applied Energy 2014;125:238-245.

[11] Cabeza L.F, Castell A, Barreneche C, de Gracia A, Fernández A.I. Materials used as PCM in thermal energy storage in buildings: A review. Renewable and Sustainable Energy Reviews 2011;15(3):1675-1695.

[12] Guillot S, Faik A, Rakhmatullin A, Lambert J, Veron E, Echegut P, Bessada C, Calvet N, Py X. Corrosion effects between molten salts and thermal storage material for concentrated solar power plants. Applied Energy 2012;94:174-181.

[13] Morales M, Navarro M.E, Fernández A. I, Martínez M, Segarra M. Instrumented indentation technique as a tool for evaluating scale formation: a study of AISI 1140 carbon Steel in molten $NaNO_3$-KNO_3 salts containing sodium chloride. In press.

[14] Esen M, Ayhan T. Development of a model compatible with solar assisted cylindrical energy storage tank and variation of stored energy with time for different phase change materials. Energy Conversion and Management 1996;37(12):1775-1785.

[15] Esen M, Durmus A, Durmus A. Geometric design of solar-aided latent heat storage depending on various parameters and phase change materials. Solar Enegy 1998;62(1):19-28.

[16] Esen M. Thermal performance of a solar-aided latent heat store used for space heating by heat pump. Solar Energy 2000;69(1):15-25.

[17] Cabeza L.F, Ibañez M, Solé C, Roca J, Nogués M. Experimentation with a water tank including a PCM module. Solar Energy Materials and Solar Cells 2006;90(9):1273-1282.

[18] Mazman M, Cabeza L.F, Mehling H, Nogues M, Evliya H, Paksoy H.Ö. Utilization of phase change materials in solar domestic hot water systems. Renewable Energy 2009;34(6):1639-1643.

[19] Gil A, Oró E, Peiró G, Álvarez S, Cabeza L.F. Material selection and testing for thermal energy storage in solar cooling. Renewable Energy 2013;57:366-371.

[20] Tyagi V.V, Buddhi D. PCM thermal storage in buildings: A state of art. Renewable and Sustainable Energy Reviews 2007;11(6):1146-1166.

[21] Oró E, de Gracia A, Castell A, Farid M.M, Cabeza L.F. Review on phase change materials (PCMs) for cold thermal energy storage applications. Applied Energy 2012;99:513-533.

[22] Sharma A, Tyagi V.V, Chen C.R, Buddhi D. Review on thermal energy storage with phase change materials and applications. Renewable and Sustainable Energy Reviews 2009;13(2):318-345.

[23] Kuznik F, David D, Johannes K, Roux J-J. A review on phase change materials

integrated in buildings walls. Renewable and Sustainable Energy Reviews 2011;15(1):379-391.
[24] Zalba B, Marín J.M, Cabeza L.F, Mehling H. Review on thermal energy storage with phase change: materials, heat transfer analysis and applications. Applied Thermal Engineering 2003;23(3):251-283.
[25] Ushak S, Gutierrez A, Flores E, Galleguillos H, Grágeda M, Vargas P. Saline waste recovery and its potential use in thermal storage. In: 1st international workshop in Lithium, Industrial minerals and Energy, IWLiME2014, Antofagasta, Chile, 2014
[26] Ushak S, Gutiérrez-Rojas A, Galleguillos H, Fernández A, Cabeza L.F, Grágeda M. Thermophysical characterization of a waste salt from the non-metallic industry as inorganic PCM. Solar Energy Materials & Solar Cells, 132(2015)385–391 .
[27] El-Sebai A.A, Al-Amir S, Al-Marzouki F.M, Faidah A, Al-Ghamdi A.A, Al-Heniti S. Fast thermal cycling of acetanilide and magnesium chloride hexahydrate for indoor solar cooking. Energy Conversion and Management. 2009;50(12):3104-3111.
[28] Li X, Gui F, Cong H, Brossia C.S, Frankel G.S. Evaluation of nitrate and nitrite reduction kinetics related to liquid-air-interface corrosion. Electrochimica Acta 2014;117:299-309.
[29] Lobsenz G., DOE confirms unprecedented waste tank leak at Hanfrod, The Energy Daily 40. 2012.
[30] Li X, Cong H, Gui F, Brossia C.S, Frankel G.S. Development of liquid-air-interface corrosion of steel in nitrate solutions. Corrosion 2014, Vol. 70, No. 3, pp. 230-246
[31] Li X, Gui F, Cong H, Brossia C.S, Frankel G.S. Examination of mechanisms for liquid-air-interface corrosion of steel for high level radioactive waste simulants. Journal of the Electrochemical Society 160;2013 C521.
[32] Jung H, Kin U, Seo G, Lee H, Lee C. Effect of dissolved oxygen (DO) on internal corrosion of water pipes. Environmental Engineering Research 2009;14(3):195-199.
[33] Seo G.T, Jung H, Lee H.D, Chung W.S, Gee C.S. Characteristics of water quality parameters on enhancing and inhibiting corrosion in water distribution system (Korean). J. Korean Soc. Environ. Eng. 1998;20(8):1151-1160.
[34] Ushak S, Davis C, Veliz S, Grágeda M. Short –term corrosion study of metallic encapsulating materials with hydrates inorganic salts in thermal energy storage systems 64th Annual Meeting of the International Society of Electrochemistry, sept. 2013
[35] Molera Solà P. Metales resistentes a la corrosión. Marcombo S.A 1990:12.

506 [36] Yoneda N, Takanashi S. Eutectic mixtures for solar heat storage. Solar Energy
507 1978;21:61-63.
508 [37] Kenisarin M.M. Short-term storage of solar energy. 1. Low temperature phase-
509 change materials. Applied Solar Energy 1993;29(2):48-65.
510
511

512 **Table 1.** Characteristics of metals sheets used in this investigation.

	Copper sheet	Aluminum sheet	Stainless steel sheet
Size [mm]	50×30	50×30	50×30
Thickness [mm]	0.1	0.1	3
Quality (grade)	C11000	A grade, alloy 1100	316L
Density [g/cm3]	8.91	2.71	7.98
Chemical composition [%]	Cu >99.90 O: 0.015-0.040	Al: 99.0-99.95 Cu: 0.05-0.20 Fe: 0.95 max Mn: 0.05 max Si: 0.95 max Zn: 0.1% max Residuals: 0.15 max	C: ≤0.03 Si: ≤1.00 Mn: ≤2.00 P: ≤0.045 S: ≤0.03 Cr: 16-18 Mo: 2-3 Ni: 12-15

513
514
515
516
517
518
519
520
521
522
523
524
525
526
527
528
529

530 **Table 2.** Mineralization of a sample of bischofite (adapted from [26]) and $MgCl_2 \cdot 6H_2O$
531 from Merck (adapted from [26]).

Compound	Bischofite (%wt.)	$MgCl_2 \cdot 6H_2O$ (%wt.)
NaCl	0.90	
KCl	0.20	
$MgCl_2 \cdot 6H_2O$	94.80	99.0-101.0
$KCl \cdot MgCl_2 \cdot 6H_2O$	1.80	
$Li_2SO_4 \cdot H_2O$	3.20	
Bromide (Br)Bromide (Br)		≤0.05≤0.05
Nitrate (NO_3), KNitrate (NO_3)		≤0.001≤0.001
PO_4, Pb, Fe, Cu, MnPhosphate (PO_4)		≤0.0005≤0.0005
Total Nitrogen (N), Al, As Sulphate (SO_4)		≤0.0002≤0.002
Ca (Calcium)Total Nitrogen (N)		≤0.003≤0.0002
Na (Sodium)Heavy metals (as Pb)		≤0.001≤0.0005
Sr (Strontium)Al (Aluminum)		≤0.005≤0.0002
Water As (Arsenic)		51.0-55.0≤0.0002
Ba (Barium)		≤0.002
Ca (Calcium)		≤0.003
Cu (Cooper)		≤0.0005
Fe (Iron)		≤0.0005
K (Potassium)		≤0.001
Mn (Manganese)		≤0.0005
Na (Sodium)		≤0.001
NH_4 (Ammonium)		≤0.002
Pb (Lead)		≤0.0005
Sr (Strontium)		≤0.005
Water		51.0-55.0

Table 3. Properties of the salt hydrates used in the experiment [26].

Sample	T_F[℃]	$\Delta_F H[J/g]$	$C_{p,solid}[kJ/(kg \cdot K)]$	$esd\ [J/cm^3]$
Bischofite	100	115	2.1	170
$MgCl_2 \cdot 6H_2O$	114.5	135	2.1	192

*esd: energy storage density

Table 4. Average percentage of mass loss of the samples upon exposure to different salts.

	Copper	Aluminum	Stainless Steel
% weight loss in $MgCl_2 \cdot 6H_2O$	23.84	8.34	0.32
% weight loss in bischofite	27.80	10.70-12.21	0.44

Table 5. Corrosion of copper, aluminum and stainless steel samples in contact with molten bischofite.

	Bischofite				
	250 h	**500 h**	**750 h**	**1000 h**	**1500 h**
Copper			Broken Piece	Broken Piece	Broken Piece
Aluminum				Broken Piece	Broken Piece
Stainless steel				n.a.	

540

541

Table 6. Corrosion of copper, aluminum and stainless steel samples in contact with molten $MgCl_2 \cdot 6H_2O$.

	$MgCl_2 \cdot 6H_2O$				
	250 h	**500 h**	**750 h**	**1000 h**	**1500 h**
Copper		Broken Piece	Broken Piece	Broken Piece	Broken Piece
Aluminum					
Stainless steel		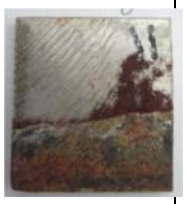		Not analysed	

Table 7. Corrosion products for each sample and respective salt found by XRD analysis.

Salt Samples	**Metal Sheet**	**Corrosion product of XRD**

$MgCl_2 \cdot 6H_2O$	Aluminum	$AlCl(OH)_2 \cdot 2H_2O / AlCl_3 \cdot 2Al(OH)_3 \cdot 6H_2O$ Aluminum chloride hydroxide hydrate
		$Mg_4Al_2(OH)_{14} \cdot 3H_2O$ Magnesium aluminum hydroxide hydrate
	Copper	$Cu_2Cl(OH)_3$ Copper oxide
		$Cu_{11}Cl_8(OH)_{14} \cdot 6H_2O$ Copper chloride hydroxide hydrate
		Cu_2O Cuprite
	Stainless Steel	Fe_2O_3 Hematite
		$Fe_8(O,OH)_{16}Cl_{1.3}$ Akaganeite-M
Bischofite	Copper	$CuCl_2 \cdot 3Cu(OH)_2$ Copper chloride hydroxide
		$(CuCl_2)(Cu(OH)_2)_3$ Copper chloride hydroxide
		Cu_2O Cuprite
	Stainless Steel	Fe_2O_3 Hematite
		$Fe(OH,Cl)_{2.55}$ Iron chloride hydroxide green rust I
	Aluminum	Amorphous product

Table 8. Summary of the elements detected via EDX in areas showed in the Figure 10.

Metal sample	**Interface area**	**Immersed area**
Copper	O, Mg, Si, S, Cl, Cu	O, Mg, Si, S, Cl, Cu
Aluminum	O, Mg, Al, S, Cl	O, Mg, Al, Cl

Stainless steel	C, O, Mg, Si, S, Cl, Cr, Mn, Fe	C, O, Mg, Si, S, Cl, Cr, Mn, Fe

575

576

577

578

579 **Table 9.** Corrosion test results for magnesium chloride hexahydrate and its mixtures.

Salt or mixture	Melting temperature, ºC	Metal sample	Observations	Corrosion rate, mg/cm^2/yr	Recommendation	Ref
Eutectic mixture $Mg(NO_3)_2 \cdot 6H_2O$ + $MgCl_2 \cdot 6H_2O$	59.1	1% Carbon steel Copper AISI-403	1000 hr; Immersed test	Considerable corrosion Considerable corrosion Nearly unchanged	No No Yes	[36,37]
Mixture 2:1 TH29 ($CaCl_2 \cdot 2H_2O$) and $MgCl_2 \cdot 6H_2O$	23	Aluminum Copper Brass Steel Stainless steel	100 days; Immersed test	0.71 0 0.68 0.59 0.58	No yes yes no yes	[8]
Mixture $Mg(NO_3)_2 \cdot 6H_2O$+ 10% $MgCl_2 \cdot 6H_2O$	75-85	Aluminum Copper Brass Carbon Steel SUS304 SUS 316	90 days; Immersed test	0.05 137 36 106 1.34 0.21	Yes No No No No Yes	[9]
$MgCl_2 \cdot 6H_2O$	116	Aluminum Stainless steel	500 melting/ solidification cycles; Immersed test	Strong corrosion Strong corrosion	no no	[21]
$MgCl_2 \cdot 6H_2O$	116	Aluminum Copper Stainless steel	63 days; Interface corrosion study	Brocken after 750 hrs Broken after 250hrs Strong corrosion	no no	Present work
Bischofite	98	Aluminum Copper Stainless steel	63 days; Interface corrosion study	Broken after 250 hrs Broken after 750hrs Strong corrosion	no no no	Present work

580

581
582
583

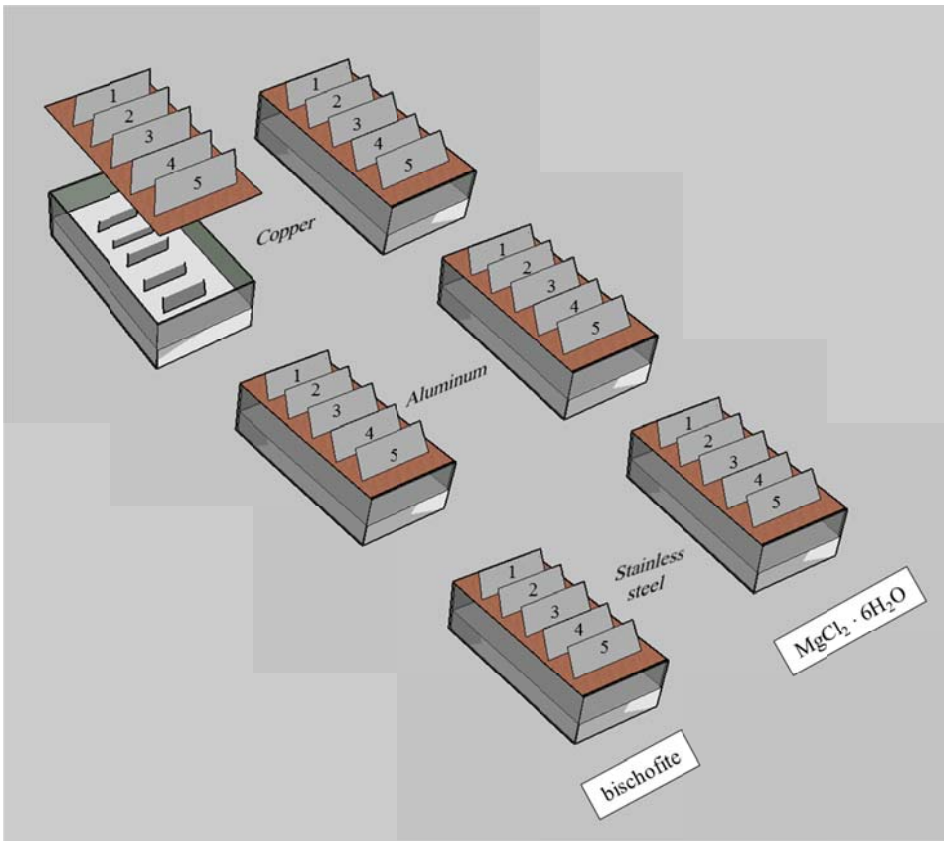

Figure 1. Schematic representation of the experiment.

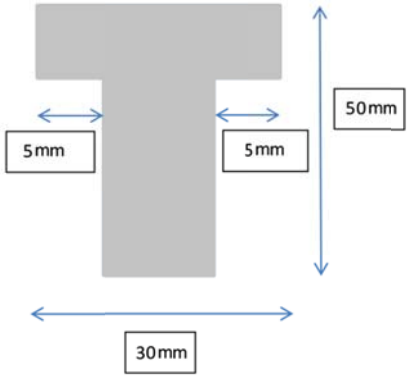

Figure 2. Dimensions of the metal samples used in the corrosion tests.

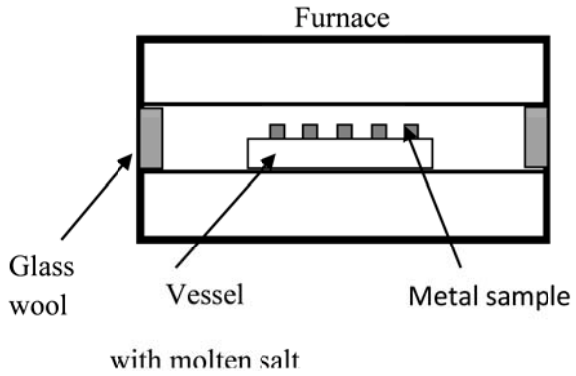

Figure 3. Schematic representation of corrosion test [34].

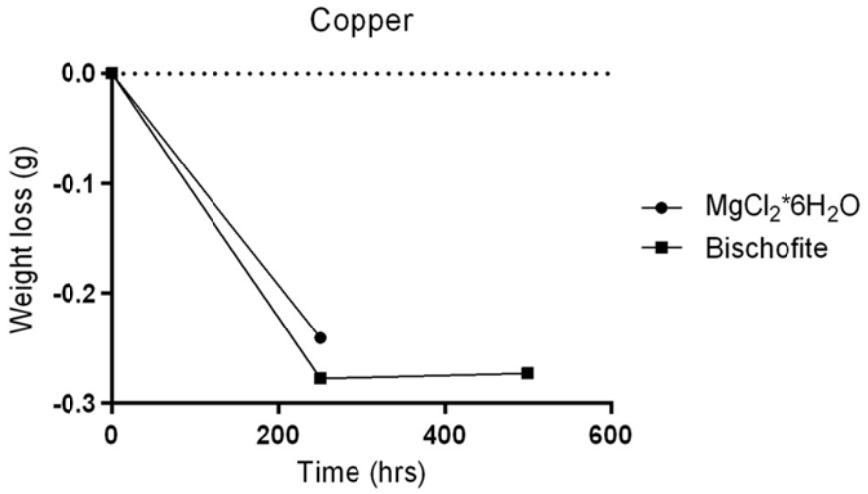

Figure 4. Weight loss for copper after being exposed to bischofite and $MgCl_2 \cdot 6H_2O$.

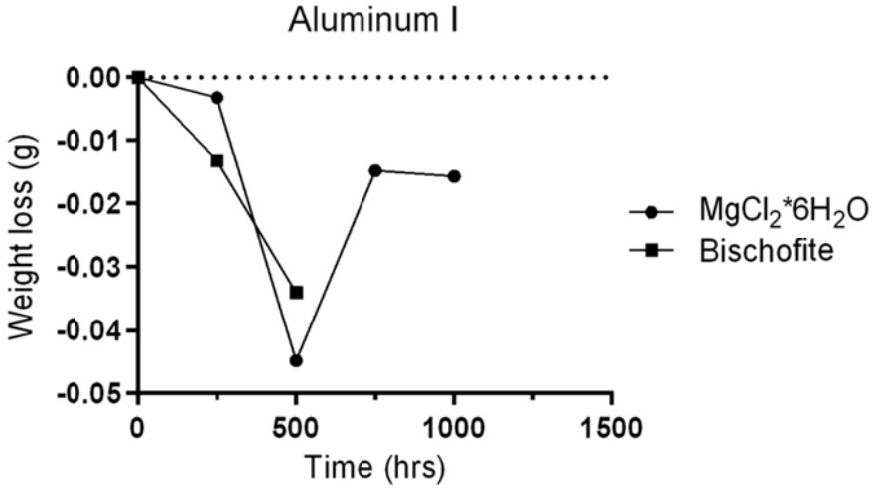

Figure 5. Weight loss for aluminum after being exposed to bischofite and $MgCl_2 \cdot 6H_2O$.

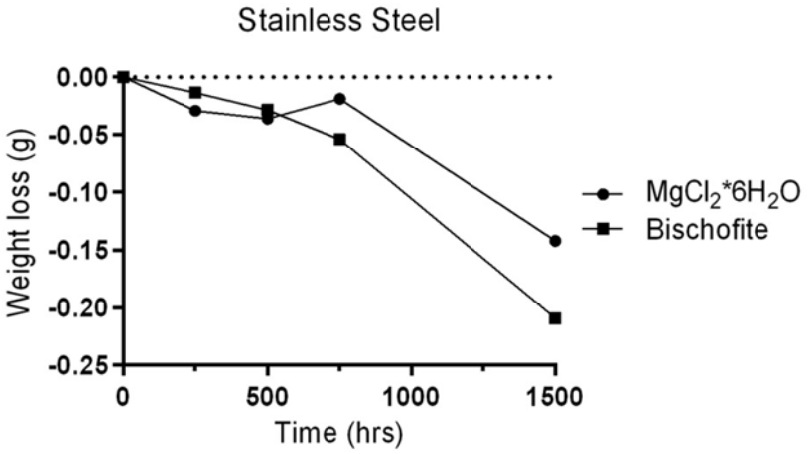

627

629 **Figure 6.** Weight loss for stainless steel after being exposed to bischofite and

630 $MgCl_2 \cdot 6H_2O$.

630

631

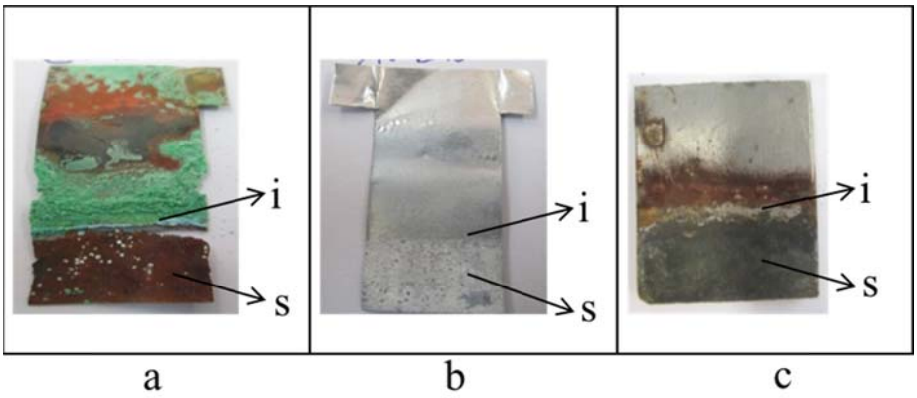

632

634 **Figure 7.** Section of the sheets where **i:** interface molten salt-air corrosion, **s:** area

635 submerged in the molten salt, for a) copper b) aluminum and c) stainless steel**.**

635

636

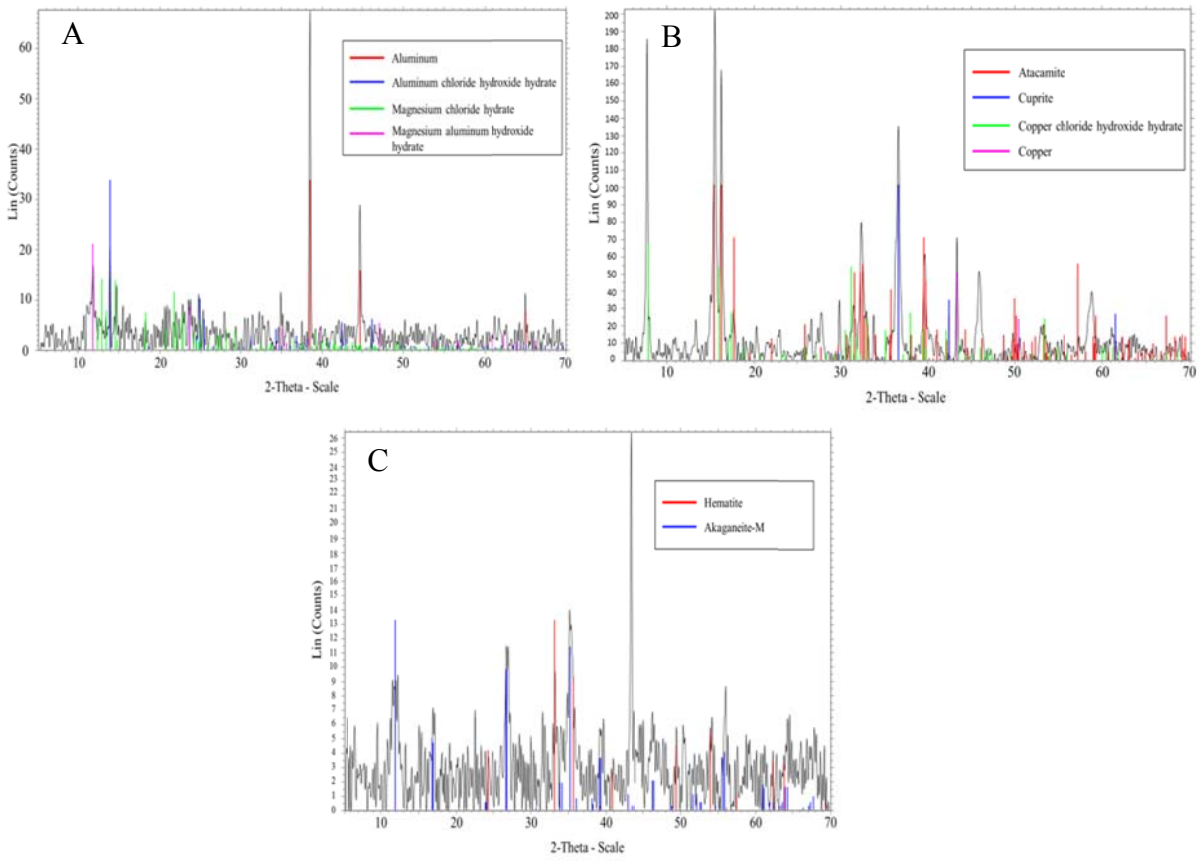

637

639 **Figure 8**. XRD diffractograms for the metal samples, **A)** aluminum **B)** copper and **C)**

640 stainless steel, immersed in $MgCl_2 \cdot 6H_2O$.

640

641

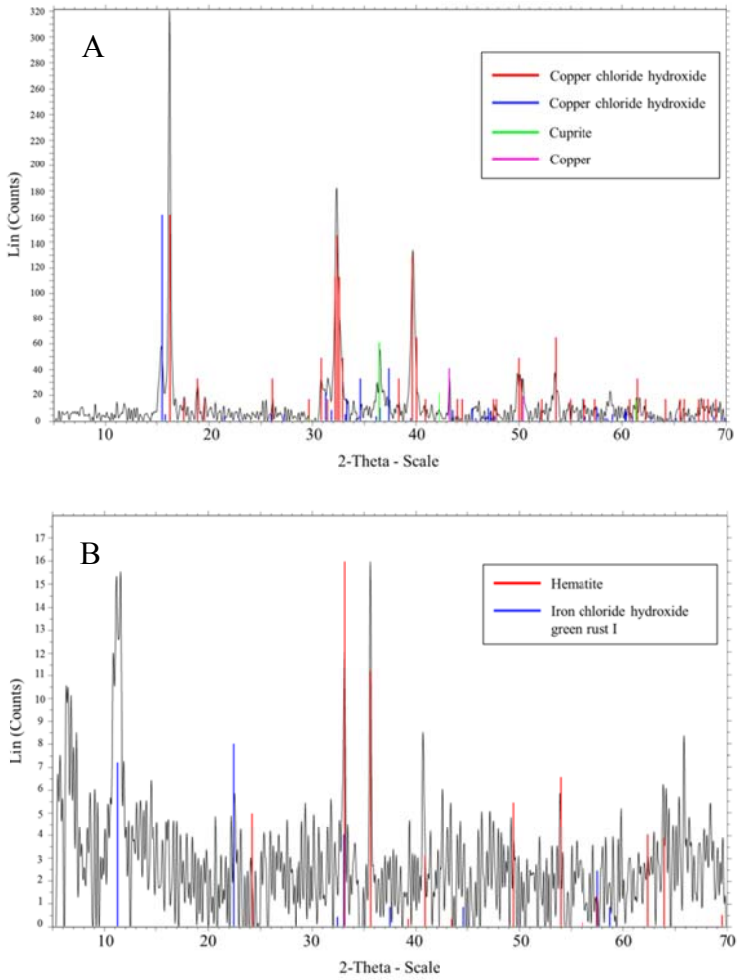

642

644 **Figure 9.** XRD diffractograms for the metal samples, **A)** copper and **B)** stainless steel,
645 immersed in bischofite.

645

646

647

648

649

650

651

652

653

654

655

656

657

250 h	Interface area	Immersed area
Stainless steel-bisch	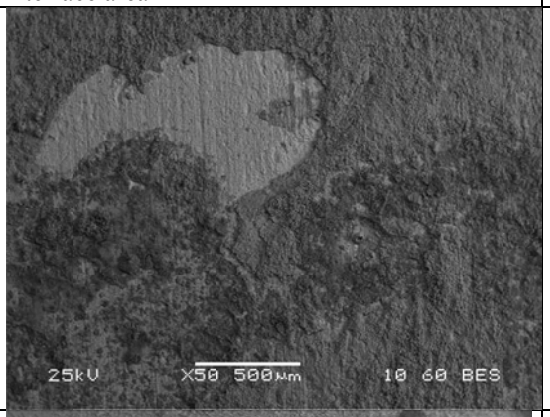	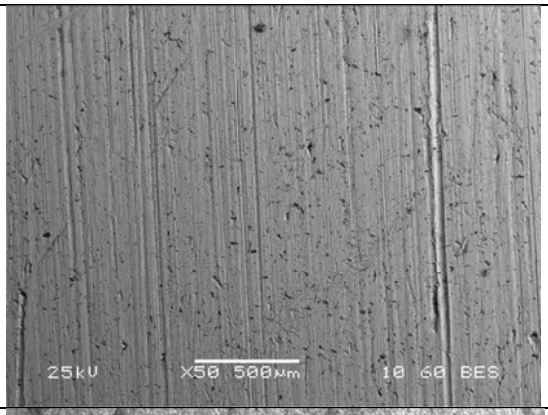
Cu-bisch	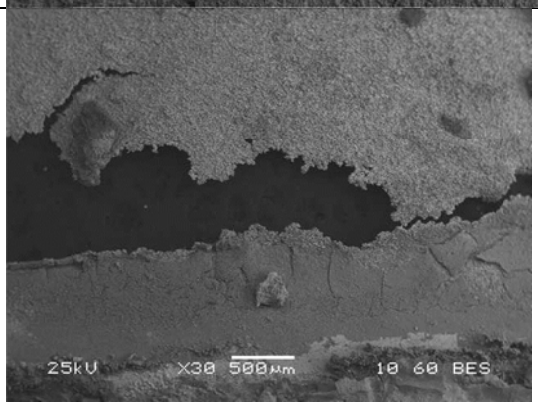	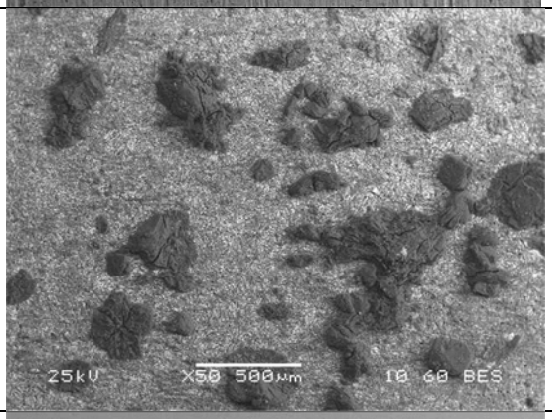
Al-bisch	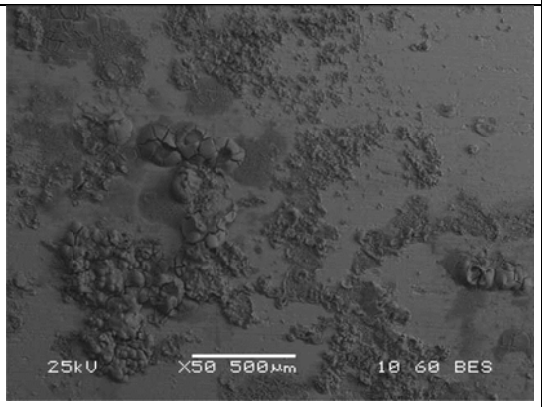	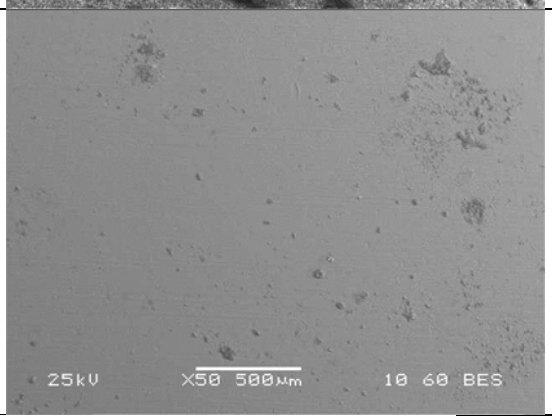

Figure 10. SEM photographs of the interface and immersed areas of stainless steel, copper and aluminum sheets treated with bischofite during 250 hrs.

	Interface area	Immersed area
250hrs	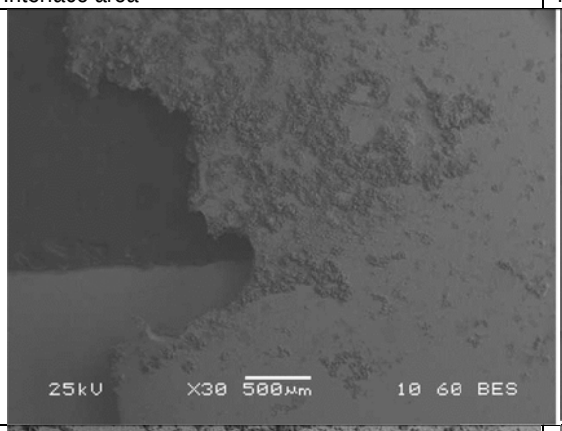	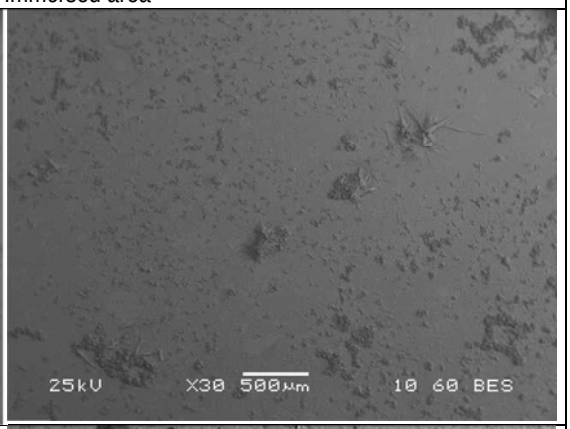
1500 hrs	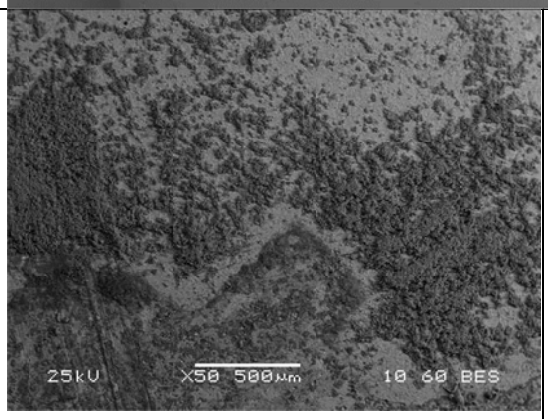	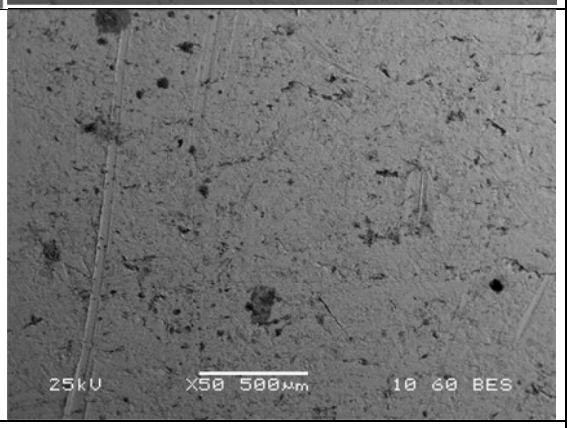

Figure 11. SEM photographs of the interface and immersed areas of aluminium sheets treated with magnesium chloride hexahydrate during 250 and 1500 hrs.